Calorimetric Study of Dynamical Heterogeneity in Blends of Polyisoprene and Poly(vinylethylene)

Tsuyoshi Sakaguchi,† Nobuyuki Taniguchi,‡ Osamu Urakawa, and Keiichiro Adachi*

Department of Macromolecular Science, Graduate School of Science, Osaka University, Toyonaka, Osaka 560-0043, Japan

Received August 21, 2004; Revised Manuscript Received November 8, 2004

ABSTRACT: The specific heat capacities C_p of blends consisting of *cis*-polyisoprene (PI) and poly(vinylethylene) (PVE) were measured in the temperature range from 80 to 320 K by using an adiabatic calorimeter. The configurational heat capacities C_{conf} of blends around the glass transition temperature T_g have been determined by subtracting the vibrational heat capacities estimated with the Einstein and Debye theories. The C_{conf} vs temperature T curves of the blends exhibit double sigmoidal increase at two glass transition temperatures T_{g1} and T_{g2} and can be resolved into two empirical sigmoidal curves. For each sigmoidal curve with the index $j = 1$ or 2, we have also determined the magnitude of the jump ΔC_j and the broadness parameter B_j of the sigmoidal curves. The dielectric relaxation spectrum for the primary process of PI/PVE blends is known to be bimodal due to dynamical heterogeneity. The relationship between the bimodal dielectric segmental relaxation and the double glass transition processes has been analyzed.

Introduction

One of conventional criteria for judging miscibility of two polymers is to observe a single glass transition for the blend by differential thermal analyses (DSC).[1−3] A similar criterion is to observe a single dielectric or viscoelastic loss peak for the primary (α) relaxation.[1−3] A more fundamental technique to determine the miscibility of components in blends is the scattering method.[1] Although these criteria have been adopted long, it was found that some miscible blends consisting of components with a large difference in the glass transition temperatures T_g do not obey these criteria and exhibit bimodal relaxation spectra due to dynamical heterogeneity.[4−8] Such a behavior leads us to expect that dynamically heterogeneous systems exhibit double glass transition. Recently, Taniguchi et al. measured heat capacities C_p on concentrated solutions of polystyrene (PS) in toluene by using an adiabatic calorimeter and found that the solutions exhibit double glass transitions.[9] Polymer/diluent systems are known to exhibit clear dynamical heterogeneity in dielectric relaxation spectra; i.e., segmental motions of polymers and motions of diluent molecules are perfectly decoupled.[10,11] Although double glass transitions have been reported for some polymer/diluent systems with thermal analyses (DSC),[11−13] there have been no reports of double glass transitions on miscible polymer blends. This paper is an extension of the study on PS/toluene solutions to a polymer blend consisting of polyisoprene (PI) and poly(vinyl ethylene) (PVE). Tomlin and Roland studied neutron scattering on blends of PI/PVE and found that the interaction parameter between PI and PVE is negative and hence PI/PVE is a perfectly miscible blend.[14] Colmenerro and co-workers[5−7] studied the dielectric behavior of PI/PVE blends and found that when the PI content is higher than 50 wt %, the segmental loss peaks due to PI and PVE are observed in distinct frequency regions. Recently, Hirose et al. also studied thermal and dielectric behavior of PI/PVE blends and observed single broad glass transition on DSC thermograms.[15] The objective of the present study is to determine accurate profiles of the heat capacity curves of PI/PVE blends around the glass transition temperature T_g. We will also examine the relationship between the calorimetric T_g and the dielectric glass transition temperature where the dielectric relaxation time becomes the time scale of measurements of the heat capacity.

Experimental Section

Materials. Polyisoprene (PI) was prepared by anionic polymerization in heptane by using *sec*-butyllithium as the initiator. The weight-average molecular weight M_w and the polydispersity M_w/M_n were determined to be 8400 and 1.08, respectively, by using a gel permeation chromatograph (GPC) equipped with a light scattering detector. The eluent was tetrahydrofuran. PVE with $M_w = 4.0 \times 10^5$ and $M_w/M_n = 1.08$ was also prepared by anionic polymerization in heptane containing 1,2-dipiperidinoethane by using *sec*-butyllithium as the initiator and characterized by using the same GPC apparatus.[16] Blends of the PI and PVE were prepared by dissolving prescribed amounts of the components in benzene, and then the solvent was removed completely under vacuum of about 10^{-2} Pa at 50 °C for 1 week.

Method. A homemade adiabatic calorimeter was used for measurements of the heat capacity C_p under constant pressure. The details of the calorimeter and the method of measurements were described previously.[9]

Results and Discussion

Heat Capacity. The temperature dependences of the specific heat capacity C_p (in J g^{-1} K^{-1}) of pure PI, pure PVE, and PI/PVE blends are shown in Figure 1.

It is seen that PI exhibits relatively sharp increase of the heat capacity C_p at T_g (= 200 K). On the other hand, PVE exhibits relatively broad jump of C_p at 265 K. Between these T_g's of the components, blends exhibit broad glass transitions. At a glance the jumps of the C_p

† Present address: Nomura Research Institute Ltd., 2-2-1, Otemachi, Chiyoda, Tokyo, Japan.
‡ Present address: Toyobo Research Center Co. Ltd., 1-1 Katata-2, Otsu, Japan.
* Corresponding author.

10.1021/ma048280g CCC: $30.25
Published on Web 12/30/2004

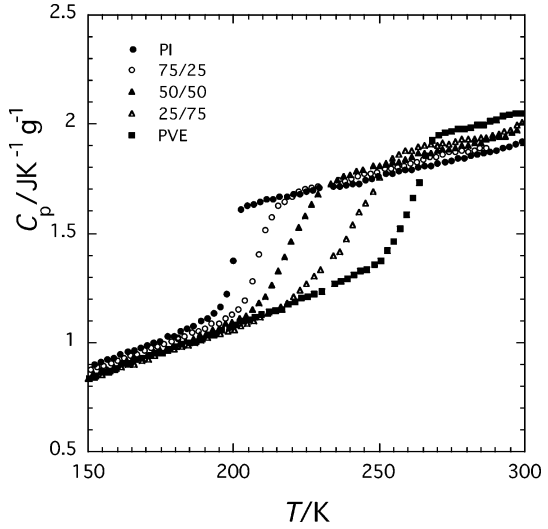

Figure 1. Specific heat capacity C_p of PI/PVE blends. The mixing ratios PI/PVE (by weight) are given in the figure.

curves of blends are similar to those of the pure components exhibiting single glass transition. However, if carefully examined, we can see that the C_p curve of PI/PVE(25/75) is double-sigmoidal.

Estimation of Vibrational Heat Capacity. Generally, the heat capacity C_p of a supercooled liquid consists of the configurational heat capacity C_{conf} and the vibrational heat capacity under constant pressure C_{p-vib}. Glass transition is a frozen-in process of the configuration and conformation of molecules, and hence in the temperature range below T_g, C_p is totally due to C_{p-vib}.[17] By representing C_{p-vib} by either a theoretical function or an empirical function, we can estimate C_{p-vib} in the range above T_g, and we can determine C_{conf} by subtracting C_{p-vib} from observed C_p. Strictly speaking, C_{conf} defined above still contains the contribution of vibrations arising from the change of vibrational frequencies due to changes in configuration. This additional contribution is approximately represented by $C_{add} = [\partial U_v(T,\Theta_D)/\partial\Theta_D][\partial\Theta_D/\partial T]$, where $U_v(T,\Theta_D)$ is the internal energy of the lattice vibrations and Θ_D the Debye temperature. Since no data of $\partial\Theta_D/\partial T$ are available, we neglected this contribution.

Although there is no clear distinction between intra modes and lattice modes in polymer molecules, we categorize C_{p-vib} into three parts: the heat capacity C_{L-vib} due to lattice vibrations, the heat capacity C_{I-vib} due to intramolecular vibrations, and $C_p - C_v$ the difference between C_p and the heat capacity under constant volume C_v. The sum $C_{L-vib} + C_{I-vib}$ is due to the harmonic vibrations and corresponds to the heat capacity under constant volume (C_{V-vib}). The correction of $C_p - C_v$ is due to the unharmonicity of the vibrations.

In the low molecular weight compounds, C_{L-vib} and C_{I-vib} can be defined without ambiguity. In the case of amorphous polymers, a lattice mode oscillating in a certain direction includes the deformations of the skeletal bonds and the intermolecular distance. Therefore, it is difficult to distinguish the skeletal modes and the lattice vibrations in amorphous polymers. Here we regard the vibrations in the monomeric unit as the intra mode and the other modes as the lattice modes. On the basis of this approximation, the monomeric unit of PI ($-C_5H_8-$) has the 33 intra modes and the 6 lattice modes. The normal-mode analysis on the PI molecule was reported by Petcavich and Coleman, who assigned

Table 1. Parameters for Calculation of Vibrational Heat Capacities

	Θ_D/K	Θ_{E1}/K	Θ_{E2}/K	Θ_{E3}/K	10^4a
PI	99	185	250	350	2.66
PVE	105	330	750	2000	0.60

the 35 modes of the PI monomer units.[18] The lowest two modes are omitted in the present analysis as they are the skeletal modes with the neighboring monomers and can be regarded as a part of lattice vibration. The contribution of the intra modes to C_p is given by the sum of the Einstein functions.[19]

Among six degrees of freedom for the lattice modes, three modes are due to the translational modes and the other three modes are due to the librational modes. The contribution of the former to C_p is approximately given by the Debye theory.[19] The contributions of the librational modes were calculated with the Einstein functions by assuming the three average frequencies ν_{liv}. The small correction of $C_p - C_v$ can be expressed by the form[20]

$$C_p - C_v = aC_{v-vib}{}^2T \tag{1}$$

where a is the constant. Those five unknown parameters, namely the Debye temperature Θ_D, the three Einstein temperatures Θ_E for the libratinal modes, and the factor a of eq 1, were estimated by a trial-and-error method so that the calculated C_p curve agrees best with the observed C_p in the temperature range below T_g. The results of thus estimated Θ_D, Θ_E, and a for PI nd PVE are listed in Table 1.

For syndiotactic PVE chains the normal-mode analysis was reported by Zerbi and Gussoni, who calculated 53 modes.[21] For the chain with the C_{2v} symmetry, selection rules predict 56 possible modes, but the frequencies of the three remaining modes were not given by Gussoni et al. Using the frequencies of those 53 modes, we calculated the vibrational heat capacity C'_{I-vib} and then assumed that the C_{I-vib} of the repeat unit is equal to the calculated C'_{I-vib}(for the 53 modes) times (56/53)/2. The slight error in this estimation may be compensated in the estimation of $C_p - C_v$ with the adjustable parameter a of eq 1. The contributions of the lattice modes were estimated on the basis of the same model as used for PI. The results are listed in Table 1.

Thus, estimated C_{p-vib}'s for PI and PVE are compared with the observed C_p in Figure 2. As is seen in these figures, the observed C_p and calculated C_p(vib) agree well with each other in the temperature range below the glass transition temperature where C_{conf} is zero.

The vibrational heat capacities of the blends were calculated by assuming the additivity of the C_{v-vib} curves:

$$C_{v-vib}(\text{PI/PVE}) = wC_{v-vib}(\text{PI}) + (1-w)C_{v-vib}(\text{PVE}) \tag{2}$$

where w is the weight fraction of PI. To calculate the weighed sum, the C_{v-vib} curves were fitted to the fourth polynomials:

$$C_{v-vib} = A + BT + CT^2 + DT^3 + ET^4 \tag{3}$$

where A, B, C, D, and E are constants and the unit of C_{v-vib} is J g^{-1} K^{-1}. The coefficients A, B, C, D, and E for PI and PVE are listed in Table 2.

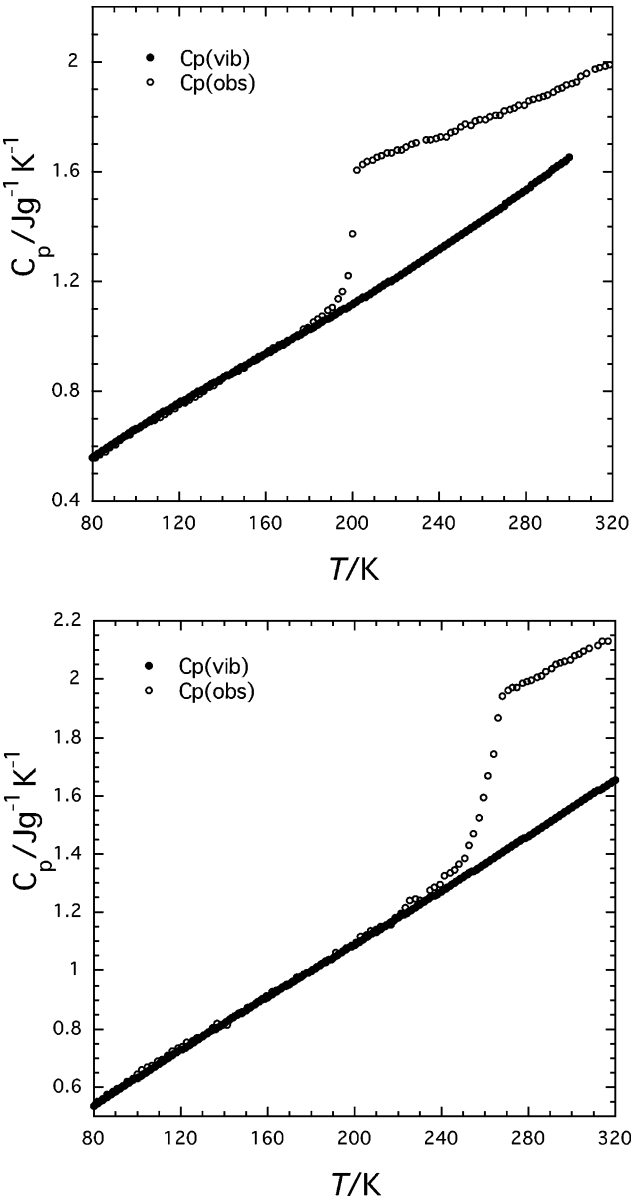

Figure 2. Comparison of observed C_p and calculated $C_{p-\mathrm{vib}}$ for PI (top) and PVE (bottom).

The assumption of additivity of $C_{v-\mathrm{vib}}$ is quite reasonable for the intramolecular vibrations since the intra modes are almost independent of intermolecular interactions. For the lattice vibration we may approximately rationalize this assumption: the density and the elastic modulus of blends are approximately linear to the composition, and hence the Debye temperature[19] of blends also changes in proportion to the composition. Thus, we calculated $C_p - C_v$ with eq 1 assuming the parameter a was adjustable. The slight error arising from the above approximation on the lattice modes can be compensated by the $C_p - C_v$.

Analyses of C_{conf}. The configurational heat capacity C_{conf} was determined by subtracting $C_{p-\mathrm{viv}}$ from the observed C_p. As reported in our previous paper[9] on the PS/toluene system, we attempted to resolve C_{conf} into two steplike curves C_1 and C_2 assuming the following empirical equation:

$$C_j \equiv \Delta C_j \frac{[1 - A_j(T - T_{gj})]\exp[B_j(T - T_{gj})]}{\exp[B_j(T - T_{gj})] + \exp[-B_j(T - T_{gj})]} \quad (4)$$

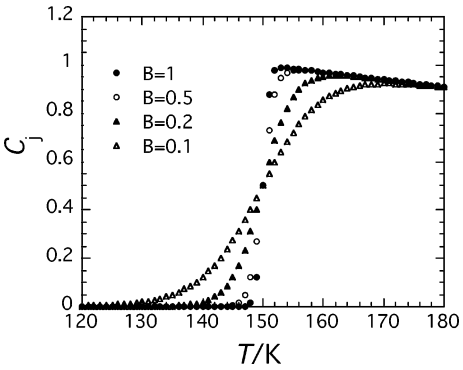

Figure 3. Model C_j curves calculated with eq 4.

Table 2. Coefficients of Eq 3

	A	10^2B	10^5C	10^7D	$10^{10}E$
PI	−0.1068	1.13011	−5.0571	1.59174	−1.5316
PVE	0.1008	0.612943	−1.07221	0.285403	−0.230598

where j is either 1 or 2 and ΔC_j, A_j, B_j, and T_{gj} are the fitting parameters. Here "1" and "2" represent the high- and low-temperature processes, respectively. Figure 4 shows the examples of the heat capacity curves calculated with eq 4 where $\Delta C_j = 1$, $A = 0.003$, $T_g = 150$, and B_j is changed as indicated in the figure. As seen in this figure, ΔC_j is the magnitude of the jump of C_j and T_{gj} is the inflection point of the sigmoidal curve and can be regarded as the glass transition temperature for the each process. B_j represents the broadness of the transition. As shown in Figure 4, the broadness increases with decreasing B. A_j is the parameter representing the negative slope of the C_j vs T curve in the range $T > T_g$. As seen in Figure 3, the model curve is almost symmetrical since A_j is small. On the other hand, the experimental configurational heat capacity is asymmetric. To include the asymmetric feature in eq 4, the function becomes more complex, and the number of parameters increases. To minimize the number of parameters, we attempted to resolve the experimental C_{conf} curves assuming eq 4.

Figure 4 shows the comparison of the observed C_{conf} and the theoretical C_{conf} calculated with eq 4 for pure PI and PVE. Asymmetric behavior of C_{conf} can be clearly seen for both polymers especially for PI. We see that C_{conf} increases rather gradually in the low-temperature side of the glass transition region and increases steeply in the high-temperature region. Such behavior cannot be represented by eq 4. PVE exhibits relatively broad glass transition, and the observed C_{conf} agrees fairly well with eq 4 although disagreement still exists. From these results, we expect that when the transition is narrow the symmetric approximation of eq 4 becomes poor, but when the transition is broad eq 4 represents well C_{conf}. In blends the glass transitions of the both components are broad, and hence eq 4 is a good approximation to represent C_{conf}. In curve fitting processes for the blends, the discrepancies in the low-temperature region of the onset of the glass transition where the asymmetric behavior appears are neglected. The error in determination of T_g due to the symmetric approximation is less than ±5 K. The error in determination of ΔC_{pi} is estimated to be less than ±10%. However, the error of B is relatively large and estimated to be ±20%.

The results of the analyses for the blends are listed in Table 3. Here we adopted the common value of A_j for processes 1 and 2. Figure 5 shows comparison of the

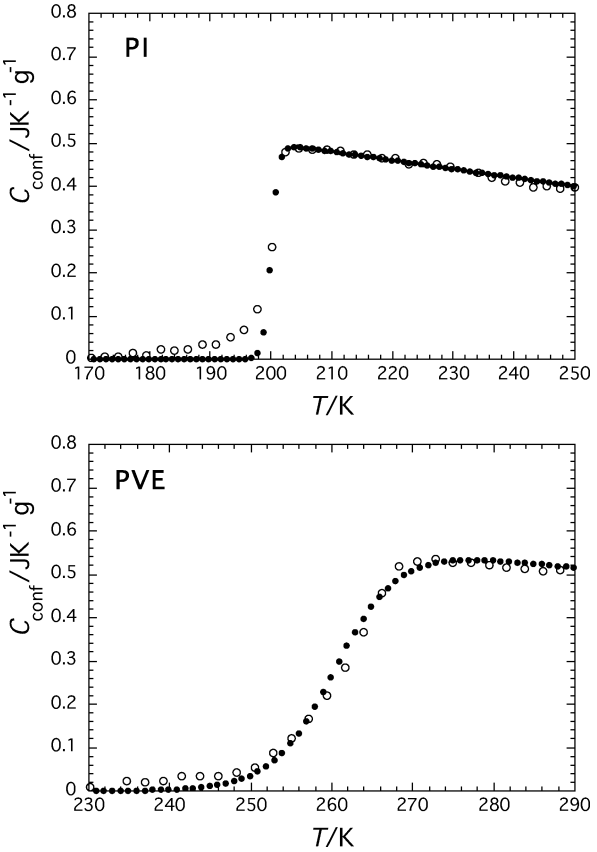

Figure 4. Comparison of observed C_{conf} and eq 4 for PI (top) and PVE (bottom). The open circles indicate observed C_{conf} and the dotted lines eq 4.

Table 3. Parameters of Eq 4 and Dielectric Glass Transition Temperatur T_D of PI/PVE Blends

	T_{g2}	T_{g1}	ΔC_{p2}	ΔC_{p1}	10^3A	B_2	B_1	T_D^{PI}	T_D^{PVE}
pure PI	200		0.50		4.0	0.8		201	
75/25	207	215	0.41	0.11	4.0	0.22	0.20	208	217
50/50	214	224	0.32	0.24	3.3	0.11	0.13		223
25/75	228	246	0.24	0.37	4.5	0.08	0.14		242
pure PVE		261		0.57	3.2		0.13		266

observed C_{conf} with the sum of thus resolved curves. It is seen that $C_1 + C_2$ agrees well with the observed C_{conf}. It is noted that the observed C_{conf} for the 50/50 blend appears to be a broad single glass transition, but as is seen in the figure, the C_{conf} curve can be resolved into two sigmoidal curves.

Figure 6 shows the composition dependence of the broadness parameters B_1 and B_2. The error bar indicates the error due to the use of symmetric eq 4. It is seen that the broadness of the T_{g2} process increases rapidly with the increase of PI content and the T_{g2} process is broader than the T_{g1} process. Similar behavior has been observed for PS/toluene solutions in which the glass transition temperature T_{g2} of toluene is lower than that of PS (T_{g1}), and B_2 decreased drastically with increasing PS content. Around T_{g2} the chains responsible for the T_{g1} process are still in a frozen-in state, and hence the molecules responsible for the T_{g2} process undergo a variety of restrictions which would be smeared out if the T_{g1} process were not frozen-in state. This phenomenon is considered to be a general phenomenon.

In Table 3 the ΔC_j changes approximately in proportion to the composition. As discussed in our previous paper,[9] the jump of the heat capacity thus resolved are much larger than the heat capacity calculated from the

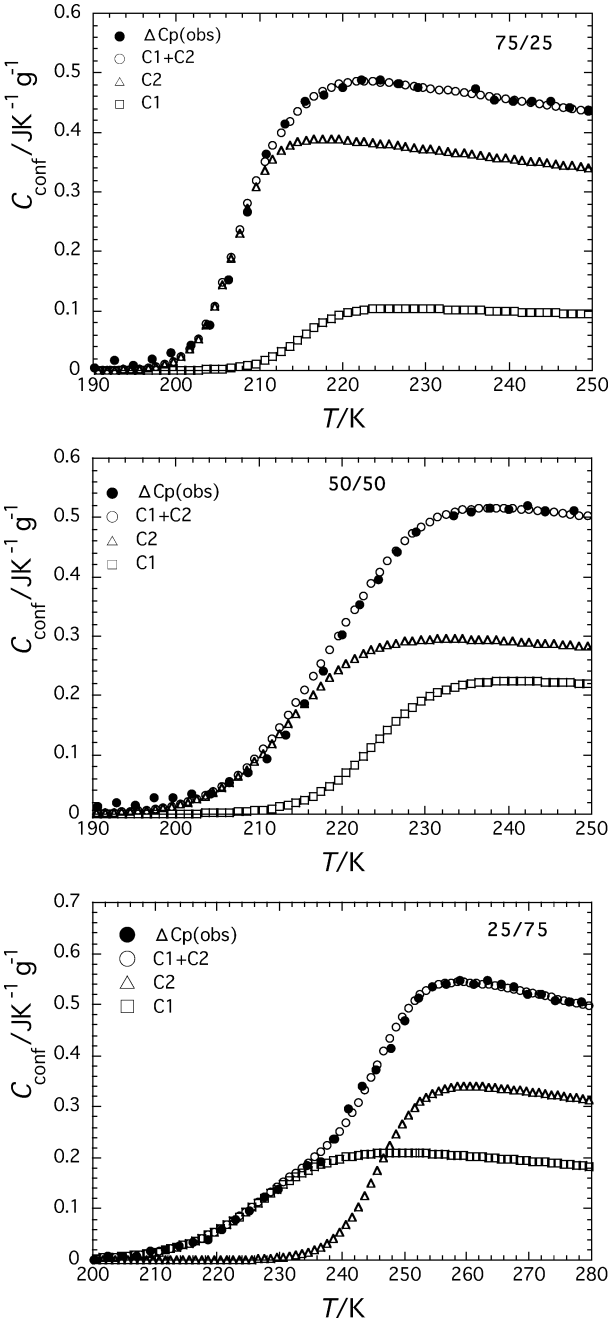

Figure 5. Configurational heat capacity $C_{conf} = C_p(\text{obs}) - C_p(\text{vib})$ of PI/PVE blends and the heat capacities C_1, C_2, and $C_1 + C_2$ calculated with eq 4: top, PI/PVE (75/25); middle, PI/PVE (50/50); bottom, PI/PVE (25/75).

energy differences among the rotational isomeric states.[22,23] Gibbs and DiMarzio explained the glass transition of polymers assuming the rotational isomeric state model.[24] Their theory is not in harmony with the present experimental results, indicating that the dominant contributino to C_{conf} is intermolecular interactions. As pointed out previously, the resolved configurational heat capacities divided by the weight fraction C_1/w_1 and C_2/w_2 correspond to the partial specific configurational heat capacities in the thermodynamic arguments.[9]

The integration of C_j/T gives changes in the configurational entropy S_{conf} of the components. According to Adam and Gibbs,[25] S_{conf} is a function of the size of cooperative region which diverges at a temperature T_2 at which S_{conf} becomes zero. This model has been employed by many authors without any clear evidence

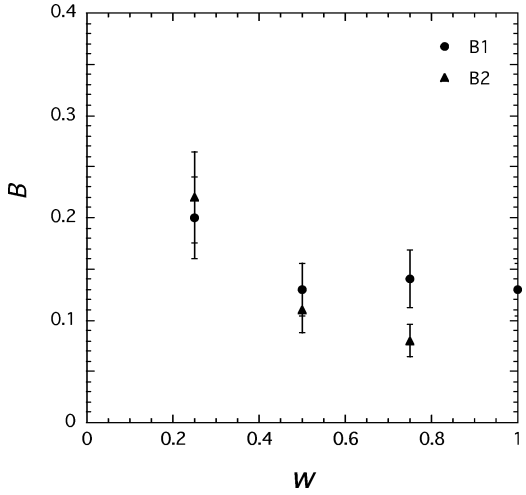

Figure 6. Dependences of B_1 and B_2 of eq 4 on the weight fraction w of PVE. Here B for pure PI (=0.80) is not plotted to magnify the plots of B for the blends.

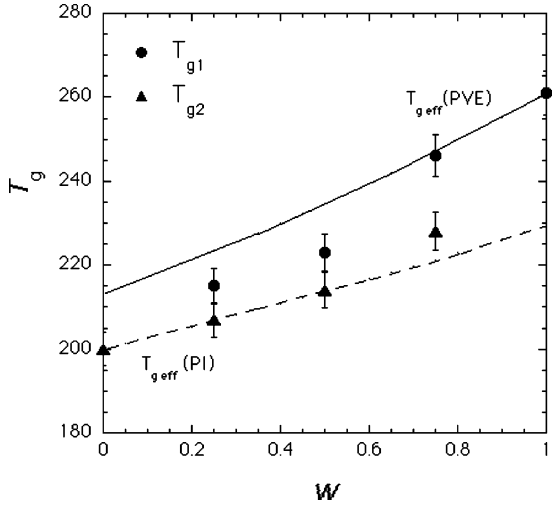

Figure 7. Dependences of T_{g1} and T_{g2} on the weight fraction w of PVE. The dotted line and solid line indicate the effective glass transition temperatures for PI and PVE, respectively.[26]

of the relationship between cooperative motions and S_{conf}. If this model is valid, there are difference of the mobility in the region of cooperative reorientation in dynamically heterogeneous systems. The relationship between the dynamical heterogeneity and cooperative rearrangement of local configuration is a future issue.

Figure 7 shows the dependence of T_{g1} and T_{g2} on the weight fraction (w_{PI}) of PI. It is seen that the separation of $T_{g1} - T_{g2}$ is shortest at $w = 0.5$. Contrarily, Hirose et al. reported that the glass transition of PI/PVE blends observed by DSC became broadest around $w = 0.5$.[15] We note in Figure 5 that the C_{conf} curve of PI/PVE(50/50) starts to increase at about 195 K and reaches equilibrium around 235 K. This width of the glass transition region (40 K) is broader than the estimate of the width (30 K) by DSC.[15] Since the sensitivity of DSC is low, we consider that the broadness of glass transition determined by the adiabatic calorimeter is similar to the broadness by DSC. We also note that in the adiabatic calorimetry the equilibrium temperatures are measured before and after input of heat. On the other hand, in DSC measurements, the sample is heated continuously. Since the heating rate in DSC is much higher than the adiabatic calorimetry, the heat conduction in DSC causes some delay of heat flow, resulting in a broader glass transition.

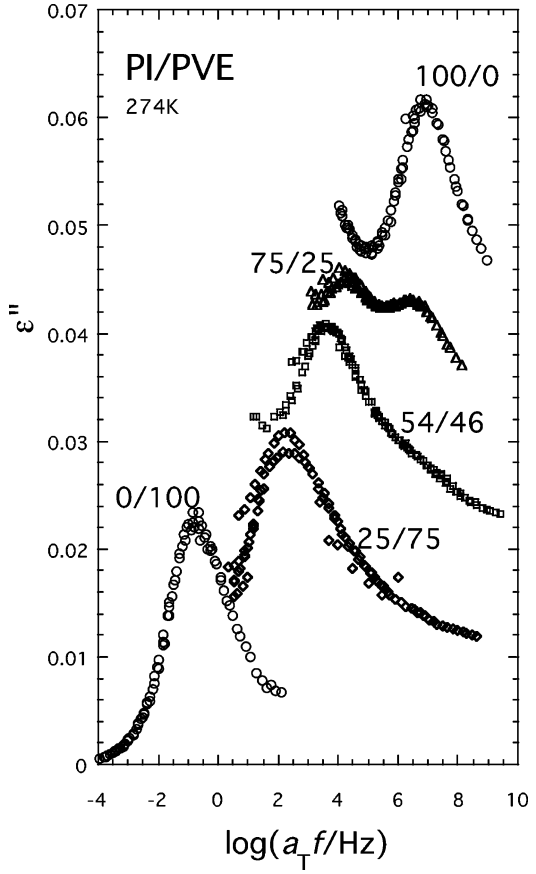

Figure 8. Master curves of ϵ'' for the segmental modes of PI/PBE blends. ϵ'' curves are shifted upward by 0.04, 0.03, 0.02, and 0.01 for blends 100/0, 75/25, 54/46, and 25/75, respectively.

Hirose et al. also reported the effective glass transition temperatures T_g^{eff} proposed by Lodge and McLeish[26] for PI/PVE blends. They determined T_g^{eff} from the dielectric segmental mode of PVE and the dielectric normal mode of PI using the WLF equation. Those T_g^{eff} values are about 5−10 K higher than the present T_{g1} and T_{g2} due to the difference of the heating rate. In Figure 7, the solid and dashed lines are theoretical T_g^{eff} for PVE and PI calculated with the Lodge−McLeish model. We will discuss this model later.

Dielectric Glass Transition Temperatures. The relaxation time τ for segmental motions becomes similar to time required for measurement of C_p at T_g. Since τ increases steeply with decreasing temperature, configurational rearrangements do not contribute to C_p below T_g and C_p changes stepwise at T_g.[27] Thus, the temperature at which τ becomes the time scale of calorimetric measurements is defined as "dielectric glass transition temperature" T_D. Since time needed for present C_p measurements was ca. 1500 s, T_D is defined as the temperature at which the loss maximum frequency $f_m = 1/(2\pi\tau)$ becomes 10^{-4} Hz.[28]

Figure 8 shows the master curves of ϵ'' for blends of PI-115 and PVE-602 reported by Hirose et al.[15] in the frequency region where the segmental mode is seen, where the code numbers 115 and 602 indicate the molecular weights in kg/mol. As is seen in this figure, the ϵ'' curve for the PI/PVE(75/25) splits into two peaks due to dynamical heterogeneity. The high- and low-frequency peaks can be assigned to the segmental modes

of PI (α_{PI}) and PVE (α_{PVE}), respectively. The Arrhrenius plots of f_m reported by Hirose et al.[15] are extrapolated with the aid of the Vogel−Fulcher equation,[29,30] and T_D^{PVE} and T_D^{PI} are determined as listed in Table 3. These temperatures agree approximately with T_{g1} and T_{g2}, indicating that T_{g1} and T_{g2} are the temperatures at which segmental motions of PVE and PI are frozen in, respectively.

Although the double glass transition is seen in the C_p curves of all blends, bimodal behavior is not seen in the ϵ'' curves for blends containing PI less than 50%. It is seen in Figure 8 that PI/PVE(54/46) blend exhibits a shoulder around log $a_T f = 7$. This behavior can be attributed to the decrease of the intensity and the broadening of the high-frequency (PI) peak with decreasing PI content.

Origin of Dynamical Heterogeneity. So far dielectric measurements have been carried out on various miscible polymer blends and polymer/diluent systems.[31−35] It has been observed in most blends that loss peaks for the primary α processes are unimodal but become much broader than those of the components. Zetsche and Fischer explained the behavior by assuming a Gaussian distribution of local concentration formed by concentration fluctuation.[31] As mentioned in the introductory section, some miscible polymer blends and polymer/diluent systems exhibit bimodal relaxation spectra. Obviously, such behavior cannot be explained by a Gaussian distribution of local concentration caused by concentration fluctuation.

Zhang et al. reported that mixtures of poly(4-vinylphenol)/poly(vinyl ethyl ether) exhibit single α relaxation in a certain composition range even though the difference of T_g of the components is as high as 185 K.[36−38] They also found that mixtures of low molecular weight phenolic compounds with poly(vinyl ethyl ether) exhibit dynamic homogeneity.[39] Those data indicate the importance of specific interactions such as hydrogen bonding on the dynamical heterogeneity. Those data indicate that the dynamical heterogeneity depends strongly on the intermolecular interactions.

In PI/PVE blends, the interactions parameter is slightly negative.[14] For such athermal systems Lodge and McLeish[26] proposed a self-concentration model. This model assumes that bimodal spectra occur due to the difference in the local friction coefficients of components arising from the difference in local concentration. The local concentration ϕ_A of the component A in a blend of A and B is higher than the average concentration ϕ due to the chain connectivity. The local volume V relevant to segmental motions of the A chains is assumed to be cube of the Kuhn step length l_K of the A chain. The same relation holds for B. The self-concentration represented by volume fraction ϕ is given by

$$\phi_s = \frac{C_\infty M_0}{k \rho N_A V} \tag{5}$$

where C_∞ is the characteristic ratio, M_0 the molecular weight of the repeat unit, k the number of backbone bonds per the repeat unit, N_A the Avogadro number, and ρ the density. Then the effective local concentration ϕ_{eff} of the A monomer unit is given by

$$\phi_{eff} = \phi_s + (1 - \phi_s)\phi \tag{6}$$

where ϕ is the average concentration of A. On account of different effective concentrations, the components A and B exhibit different effective glass transition at T_{gA}^{eff} and T_{gB}^{eff}, respectively. Assuming the Fox equation T_g^{eff} is given by replacing ϕ by ϕ_{eff}. The values of T_g^{eff} for PI and PVE have been determined with ϕ_s reported by Lodge and McLeish (ϕ_s for PI = 0.45 and ϕ_s for PVE = 0.25).[26] The results are compared with T_{g1} and T_{g2} in Figure 7 by replacing ϕ with w. It is seen that T_g^{eff} for PI agrees approximately with T_{g2}, but T_{g1}does not agree with T_g^{eff} for PVE. Recently, Haley et al. tested the self-concentration model for PI/PVE blends using various dynamic methods.[40] They also concluded that the model describes quantitatively the behavior for PI but does not for PVE.

Above discussion leads us to conclude that the dominant factor governing dynamic heterogeneity depends on the chemical natures of components. It is expected that with increasing intermolecular interactions the components of a miscible system move cooperatively and dynamical heterogeneity is enhanced in the systems with weak interactions. From the polymer/solvent systems we also note that difference in the sizes of components enhances dynamic heterogeneity.

Conclusion

The heat capacities C_p of PI/PVE blends have been measured by using an adiabatic calorimeter. The configurational heat capacity C_{conf} vs temperature T curves of PI/PVE blends can be resolved into two sigmoidal curves C_1 and C_2. The glass transition temperatures T_{g1} and T_{g2} ($T_{g1} > T_{g2}$) for the two sigmoidal curves have been determined by assuming an empirical equation. The dielectric relaxation spectra for the segmental mode split into the α_{PVE} and α_{PI} peaks when the PI content is high. T_{g1} and T_{g2} agree with the dielectric glass transition temperatures T_{PVE} and T_{PI}, which are defined as the temperatures at which the dielectric relaxation times for the α_{PVE} and α_{PI} processes become 10^3 s, respectively. This indicates that T_{g1} and T_{g2} are glass transition temperatures at which segmental motions of PVE and PI are frozen in, respectively. We conclude that dynamically heterogeneous systems composed of mobile and less mobile components exhibit glass transition at different temperatures. The broadness of the glass transition for the T_{g2} process for PI increased drastically with increasing PVE content.

References and Notes

(1) Olabisi, O.; Robeson, L. M.; Shaw, M. T. *Polymer−Polymer Miscibility*; Academic Press: New York, 1979.
(2) Runt, J. R. In *Dielectric Spectroscopy of Polymeric Materials*; Runt, J. P., Fitzgerald, J. J., Eds.; American Chemical Society: Washington, DC, 1997; Chapter 10; pp 283−302.
(3) Utracki, L. A. *Polymer Alloys and Blends Thermodynamics and Rheology*; Hanser Publishers: New York, 1990.
(4) Roland, C. M.; Ngai, K. L. *Macromolecules* **1992**, *25*, 363.
(5) Algeria, A.; Colmenero, J.; Ngai, K. L.; Roland, C. M. *Macromolecules* **1994**, *27*, 4486.
(6) Alvarez, F.; Alegria, A.; Colmenero, J. *Macromolecules* **1997**, *30*, 597.
(7) Arbe, A.; Alegria, A.; Colmenero, J.; Hoffman, S.; Willner, L.; Richter, D. *Macromolecules* **1999**, *32*, 7572.
(8) Urakawa, O.; Fuse, Y.; Hori, H.; Qui, T.; Yano, O. *Polymer* **2001**, *42*, 765.
(9) Taniguchi, N.; Urakawa, O.; Adachi, K. *Macromolecules*, in press.
(10) Yoshizaki, K.; Urakawa, O.; Adachi, K. *Macromolecules* **2003**, *36*, 2349.
(11) Adachi, K.; Ishida, Y. *Polym. J.* **1979**, *11*, 233.
(12) Ceccorulli, G.; Pizzori, M.; Scandola, M. *Polymer* **1987**, *28*, 2077.

(13) Savin, D. A.; Larson, A. M.; Lodge, T. P. *J. Polym. Sci., Part B: Polym. Phys. Ed.* **2004**, *42*, 1155.
(14) Tomlin, D. W.; Roland, C. M. *Macromolecules* **1992**, *25*, 2994.
(15) Hirose, Y.; Urakawa, O.; Adachi, K. *Macromolecules* **2003**, *36*, 3699.
(16) Halasa, A. F.; Lohr, D. F.; Hall, J. E. *J. Polym. Sci., Part A: Polym. Chem. Ed.* **1981**, *42*, 1155.
(17) Shen, M. C.; Eisenberg, A. *Prog. Solid State Chem.* **1967**, *3*, 407.
(18) Petcavich, R. J.; Coleman, M. M. *J. Polym. Sci., Part A: Polym. Chem. Ed.* **1980**, *18*, 2097.
(19) Kittel, C. *Introduction to Solid State Physics*; Wiley: New York, 1953; Chapter 6.
(20) Nersnst, W.; Lindemann, F. *Electrochemistry* **1911**, *17*, 817.
(21) Zerbi, G.; Gussoni, M. *Spectrochim. Acta* **1966**, *22*, 2111.
(22) Roe, R.-J.; Tonelli, A. E. *Macromolecules* **1978**, *11*, 114.
(23) Yoon, D. Y.; Sundararajan, P. R.; Flory, P. J. *Macromolecules* **1975**, *8*, 776.
(24) Gibbs, J. H.; DiMarzio, E. A. *J. Chem. Phys.* **1958**, *28*, 373.
(25) Adam, G.; Gibbs, J. H. *J. Chem. Phys.* **1965**, *43*, 139.
(26) Lodge, T. P.; McLeish, T. C. B. *Macromolecules* **2000**, *33*, 5278.
(27) Shen, M. C.; Eisenberg, A. *Prog. Solid State Chem.* **1967**, *3*, 407.
(28) Kauzmann, W. *Chem. Rev.* **1948**, *43*, 219.
(29) Vogel, H. *Phys. Z.* **1921**, *22*, 645.
(30) Fulcher, G. A. *J. Am. Ceram. Soc.* **1925**, *8*, 339.
(31) Zetsche, A.; Fischer, E. W. *Acta Polym.* **1994**, *45*, 168.
(32) Katana, G.; Fischer, E. W.; Hack, Th.; Abetz, V.; Kremer, F. *Macromolecules* **1995**, *28*, 2714.
(33) Hayakawa, T.; Adachi, K. *Macromolecules* **2000**, *33*, 6834.
(34) Yada, M.; Nakazawa, M.; Urakawa, O.; Morishima, Y.; Adachi, K. *Macromolecules* **2000**, *33*, 3368.
(35) Nakazawa, M.; Urakawa, O.; Adachi, K. *Macromolecules* **2000**, *33*, 7898.
(36) Zhang, S. H.; Painter, P. C.; Runt, J. *Macromolecules* **2002**, *35*, 9403.
(37) Zhang, S. H.; Jin, X.; Painter, P. C.; Runt, J. *Macromolecules* **2003**, *36*, 5710.
(38) Jin, X.; Zhang, S. H.; Runt, J. *Macromolecules* **2003**, *36*, 8033.
(39) Zhang, S. H.; Jin, X.; Painter, P. C.; Runt, J. *Macromolecules* **2003**, *36*, 7179.
(40) Haley, J. C.; Lodge, T. P.; He, Y.; Ediger, M. D.; von Meerwall, E. D.; Mijovic, J. *Macromolecules* **2003**, *36*, 6142.

MA048280G